Proceedings of IDETC'05
2005 ASME International Design Engineering Technical Conferences and
Computers and Information in Engineering Conference
Long Beach, California, USA, September 24-28, 2005

DETC2005-84388

COMPLICATED REGULAR AND CHAOTIC MOTIONS OF THE PARAMETRICALLY EXCITED PENDULUM

Eugene I. Butikov
St. Petersburg State University
198904 St. Petersburg, Russia
Email: butikov@spb.runnet.ru

ABSTRACT

Several new types of regular and chaotic behavior of the parametrically driven pendulum are discovered with the help of computer simulations. A simple physical explanation is suggested to the phenomenon of subharmonic resonances. The boundaries of these resonances in the parameter space and the spectral composition of corresponding stationary oscillations are determined theoretically and verified experimentally. A close relationship between the upper limit of stability of the dynamically stabilized inverted pendulum and parametric resonance of the non-inverted pendulum is established. Most of the newly discovered modes are still waiting a plausible physical explanation.

1 Introduction

Simple dynamical systems for which our intuition may seem to be well developed can behave in very complicated and even irregular ways. This occurs in spite of exact nature of governing physical laws and deterministic character of relevant differential equations.

This paper examines different kinds of extraordinary behavior of a parametrically driven pendulum – a simple system which serves a paradigm to contemporary nonlinear physics. Additionally, the differential equation for the pendulum is frequently encountered in various branches of science and engineering.

Depending on the excitation frequency and amplitude of the pendulum pivot point, this seemingly simple system exhibits a rich variety of nonlinear phenomena characterized by amazingly different types of motion. Some modes of such parametrically forced pendulum are quite simple indeed and agree well with our intuition, while others are very complicated and counterintuitive. Although after Stephenson [1] this system has been permanently investigated during almost a century, a lot of new modes of its regular and chaotic motions are discovered only recently.

An interesting feature in the behavior of the parametrically driven rigid pendulum is the dynamic stabilization of its inverted position. This intriguing system, widely known as "Kapitza's pendulum" [2], attracted attention of many researchers, and the theory of the phenomenon may seem to be well elaborated (see, for example, [3]). Nevertheless, more and more new features in its behavior are reported regularly [4] – [12], [20]. Among recent new discoveries the most significant are the destabilization of the (dynamically stabilized) inverted position at large driving amplitudes through excitation of period-2 ("flutter") oscillations [9]- [10], and the existence of *n*-periodic "multiple-nodding" regular oscillations [19].

Behavior of the pendulum whose axis is forced to oscillate with a frequency from certain intervals (and with large enough amplitude) can be chaotic. The pendulum makes several revolutions in one direction, then swings for a while with permanently changing amplitude, then rotates again in the former or in the opposite direction, and so forth. For other values of the driving frequency and/or amplitude, the chaotic motion can be purely oscillatory, without revolutions. For example, the pendulum can make one oscillation during each two driving periods, but in each next cycle the motion (the phase orbit) is slightly (and randomly) different from the previous cycle. Chaotic modes of the parametrically driven pendulum have been intensively investigated over past decades [13] – [18].

The overwhelming majority of publications related to the parametrically driven pendulum are highly mathematical in nature and sometimes obscure the physical nature of the phenomenon under investigation. We present in this paper quite simple qualitative physical explanations for several extraordinary modes of its regular behavior. In particular, we show that the excitation of period-2 "flutter" mode is closely related with the commonly known conditions of parametric instability for the non-inverted pendulum, and that the so-called "multiple-nodding" oscillations (which exist for both the inverted and downward positions) can be treated as high order subharmonic resonances of the parametrically driven pendulum. The spectral composition of the subharmonic resonances in the low-amplitude limit is investigated quantitatively, and the boundaries of the region in the parameter space are determined in which these resonances can exist. The conditions of the inverted pendulum stability are determined with a greater precision compared to the previous results.

Several new types of regular and chaotic behavior are reported for the parametrically driven pendulum, expanding this beautiful collection. The new modes were discovered with the help of computer simulations. Most of these modes are rather exotic and counterintuitive. They are still waiting a plausible physical explanation. Understanding such complicated behavior of this simple system is certainly a challenge to our physical intuition.

2 The Physical System

For simplicity we consider a light rigid rod of length l with a heavy small bob of mass m on its end and assume that the rod has zero mass, so that all the mass of the pendulum is concentrated in the bob. The force of gravity $m\mathbf{g}$ provides a restoring torque, given by $-mgl\sin\varphi$, with a value proportional to the sine of angular deflection φ of the pendulum from the equilibrium position. When the axis of the pendulum is constrained to move with acceleration along the vertical line, it is convenient to analyze the motion in the non-inertial frame of reference associated with this axis. Due to the acceleration of this frame the force of inertia $-m\ddot{z}$ is added to the force of gravity, where $z(t)$ is the time-dependent vertical coordinate of the axis. The torque of this force $-m\ddot{z}l\sin\varphi$ must be added to the differential equation for $\varphi(t)$.

If the axis of the pendulum is forced to execute a given harmonic oscillation along the vertical line with a frequency ω and an amplitude a,

$$z(t) = a\sin\omega t \quad \text{or} \quad z(t) = a\cos\omega t, \tag{1}$$

the force of inertia $F_{\text{in}}(t)$ exerted on the bob also has a sinusoidal dependence on time. This force is directed downward during the time intervals for which $z(t) < 0$ (i.e., when the axis is below the middle point of its oscillations), which is equivalent to some strengthening of the force of gravity, and upward when the axis is over the middle point, which is equivalent to some weakening of the gravitational force. When the frequency and/or amplitude of the pivot are large enough (when $a\omega^2 > g$), for some part of the period the apparent gravity is even directed upward.

On the basis of this approach, taking into account the periodic variations of the apparent gravity, we can easily explain, say, the physical reason for the ordinary parametric swinging of the pendulum, when its pivot is driven vertically with a frequency approximately twice the frequency of natural oscillations. The time variations of the force of inertia give a clear physical explanation to the growth of initially small oscillations at conditions of parametric resonance. When the oscillating pivot is below its middle position, this additional force is directed downward, and vice versa. We can treat the effect of this varying force as a periodic modulation of the gravitational force. Let the pendulum move from the utmost deflection toward the lower equilibrium position while the pivot in its constrained oscillation is below the mid-point. Due to the additional apparent gravity the pendulum gains a greater speed than it would have gained in the absence of the pivot's motion. During the further motion of the pendulum away from the equilibrium position, the pivot is above its mid-point, so that the force of inertia reduces the apparent gravity. Thus the pendulum reaches a greater angular displacement than it would have reached otherwise. During the second half-period of the pendulum's motion the swing increases again, and so on, until the stationary motion is established due to violation of the resonance conditions at large swing.

The simulation of the system is based on numerical integration of the exact differential equation for the momentary angular deflection $\varphi(t)$. This equation includes, beside the torque of the force of gravity, the instantaneous value of the torque exerted on the pendulum by the force of inertia that depends explicitly on time t:

$$\ddot{\varphi} + 2\gamma\dot{\varphi} + \omega_0^2\left(1 - \frac{a}{l}\frac{\omega^2}{\omega_0^2}\cos\omega t\right)\sin\varphi = 0. \tag{2}$$

The second term takes into account the braking frictional torque, assumed to be proportional to the momentary angular velocity $\dot{\varphi}$ in the mathematical model of the simulated system. The damping constant γ is related to the dimensionless quality factor Q characterizing the role of viscous friction: $Q = \omega_0/2\gamma$.

We note that oscillations about the inverted position can be formally described by the same differential equation, Eqn. (2), with negative values of ω_0^2. In other words, we can consider $\omega_0^2 = g/l$ in Eqn. (2) as a control parameter whose variation is physically equivalent to changing the gravitational force mg exerted on the pendulum. When this control parameter is diminished through zero to negative values, the constant (gravitational) torque in Eqn. (2) first turns to zero and then changes its sign to the opposite. Such a "gravity" tends to bring the pendulum into the inverted position $\varphi = \pi$, destabilizing the downward position $\varphi = 0$ of the unforced pendulum: if in Eqn. (2) $\omega_0^2 < 0$, the inverted position is equivalent to the downward position with the positive value of ω_0^2 of the same magnitude.

The force of inertia, arising due to constrained oscillations of the axis, explains, in particular, the pendulum stabilization in the inverted position. Details of the physical mechanism responsible for the dynamical stabilization of the inverted pendulum can be found in [20]. The principal idea is utterly simple: Although the mean value of the force of inertia $F_{\text{in}}(t)$, averaged over the short period of these oscillations, is zero, the averaged over the period value of its *torque* about the axis is not zero. Figure 1 explains the origin of this torque.

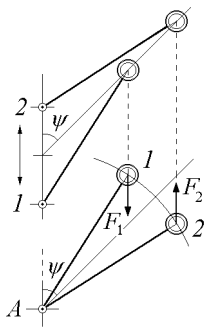

Figure 1. Positions of the pendulum rod and the forces of inertia F_1 and F_2, exerted on the pendulum in the non-inertial reference frame (lower part of the figure) at the extreme positions *1* and *2* of the oscillating axis *A*.

When the axis is displaced downward (to position *1*) from its mid-point, the force of inertia F_1 exerted on the bob is also directed downward. In the other extreme position *2* the force of inertia F_2 has an equal magnitude and is directed upward (see figure 1). However, the torque of the force of inertia in position *2* is greater than in position *1* because the *arm* of the force in this position is greater. Also the mean (averaged over the period) value of the torque is not zero. The reason is that both the force $F_{\text{in}}(t)$ and the *arm* of this force vary with time in the same way synchronously with the axis' vibrations. This non-zero mean torque tends to align the pendulum along the direction of forced oscillations of the axis. For given values of the driving frequency and amplitude, the mean torque of the force of inertia depends only on the mean angle ψ of the pendulum's deflection from the direction of the pivot's vibration.

We can consider the angular motion of the pendulum $\varphi(t)$ as a superposition of two components: a "fast" (or "vibrational") component, and "slow" or "smooth" component described by the angle $\psi = \langle\varphi(t)\rangle$, whose variation during a period of constrained vibrations is small. If we use a stroboscopic illumination with a short interval between the flashes that equals the period of constrained vibrations of the pendulum's axis, we can see only this slow component of the motion. This motion can be described by a slow-varying function $\psi(t)$ satisfying the following approximate differential equation if friction is ignored (see [20]):

$$\ddot{\psi} = -\omega_0^2 \sin\psi - \frac{1}{2}\frac{a^2}{l^2}\omega^2 \cos\psi \sin\psi. \tag{3}$$

We can introduce an effective potential $U(\psi)$ that governs the smooth motion of the pendulum averaged over the rapid oscillations. This potential consists of two parts $U_{\text{gr}}(\psi)$ and $U_{\text{in}}(\psi)$ that describe the influence of the force of gravity and the force of inertia respectively:

$$U(\psi) = U_{\rm gr}(\psi) + U_{\rm in}(\psi) = mgl(1-\cos\psi) + \frac{1}{4}ma^2\omega^2(1-\cos 2\psi). \tag{4}$$

This effective potential was first introduced by Landau [3], and derived by various different methods afterwards (see, for example, [11], [12], or [20]). The graphs of $U_{\rm gr}(\psi)$ and $U_{\rm in}(\psi)$ are shown in Fig. 2. They both have a sinusoidal shape, but the period of $U_{\rm in}(\psi)$ is just one half of the period of $U_{\rm gr}(\psi)$. Their minima at $\psi = 0$ coincide, thus generating the principal minimum of the total potential function $U(\psi) = U_{\rm tot}(\psi)$. This minimum corresponds to the stable lower equilibrium position of the pendulum. But the next minimum of $U_{\rm in}(\psi)$ is located at $\psi = \pi$, where $U_{\rm gr}(\psi)$ has its maximum corresponding to the inverted position of the pendulum.

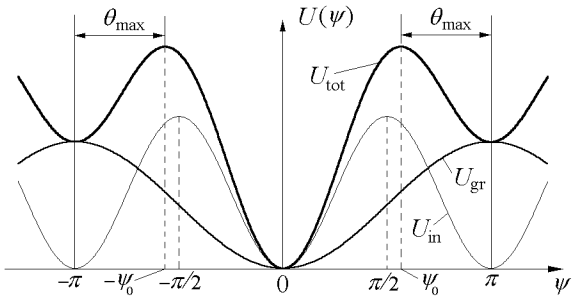

Figure 2. Graphs of the gravitational potential energy $U_{\rm gr}$, mean potential energy $U_{\rm in}$ in the field of the force of inertia, and of the total potential energy $U_{\rm tot}(\psi)$ for the pendulum with an oscillating axis ($a^2\omega^2/gl = 4.8$).

As follows from (4) or (3), the mean torque of the force of inertia can exceed in magnitude the torque of the gravitational force tending to tip the pendulum down, when the following condition is fulfilled:

$$a^2\omega^2 > 2gl. \tag{5}$$

When this criterion of dynamical stabilization, Eqn. (5), is fulfilled, the maximum admissible angular deflection from the inverted vertical position $\theta_{\max} = \pi - \psi_0$ for which the pendulum will return to this position, is given by the following equation (valid for any values of $\theta_{\max}$ that do not exceed $\pi/2$):

$$\cos\theta_{\max} = -\cos\psi_0 = \frac{2gl}{a^2\omega^2} = 2\left(\frac{\omega_0}{\omega}\frac{l}{a}\right)^2. \tag{6}$$

Being deflected from the downward vertical position (and from the upward by an angle that does not exceed $\theta_{\max}$), the pendulum will execute relatively slow oscillations about this equilibrium position. This motion can be described by a slow-varying function $\psi(t)$ satisfying differential equation (3). The frequencies $\omega_{\rm up}$ and $\omega_{\rm down}$

of small slow oscillations about the inverted position and the lower vertical position are given by the following expressions:

$$\omega_{\text{up}}^2 = \frac{1}{2}\left(\frac{a}{l}\right)^2 \omega^2 - \omega_0^2, \qquad \omega_{\text{down}}^2 = \frac{1}{2}\left(\frac{a}{l}\right)^2 \omega^2 + \omega_0^2. \tag{7}$$

Substituting $\omega_0 = 0$ into these formulas, we get the expression $\omega_{\text{slow}} = \omega(a/l)/\sqrt{2}$, valid at $a/l \ll 1$ for the frequency of small slow oscillations of the pendulum with vibrating axis in the absence of the gravitational force.

3 Subharmonic resonances of high orders

The natural slow oscillatory motion in the effective potential well is almost periodic (exactly periodic in the absence of friction). Executing these damped slow oscillations, the pendulum gradually approaches the equilibrium position (either dynamically stabilized inverted position or ordinary downward position). However, when the driving amplitude and frequency lie within certain ranges, the pendulum can be trapped in a *n*-periodic limit cycle locked in phase to the rapid forced vibration of the axis. In such oscillations the phase trajectory repeats itself after *n* driving periods T. Since the motion has period nT, and the frequency of its fundamental harmonic equals ω/n (where ω is the driving frequency), this phenomenon can be called a subharmonic resonance of *n*-th order. For the inverted pendulum with a vibrating pivot, periodic oscillations of this type were first described by Acheson [19], who called them "multiple-nodding" oscillations.

Such oscillations, which are synchronized with the excitation frequency, can occur also about the downward position and, in the absence of gravity, about any of the two equivalent dynamically stabilized equilibrium positions (see [21]). An example of such stationary oscillations whose period equals eight periods of the axis is shown in Fig. 3.

The left-hand upper part of the figure shows the spatial trajectory of the pendulum's bob at these multiple-nodding oscillations. The left-hand lower part shows the closed looping trajectory in the phase plane (φ, $\dot{\varphi}$). Right-hand side of Fig. 3, alongside the graphs of $\varphi(t)$ and $\dot{\varphi}(t)$, shows also their harmonic components and the graphs of the pivot oscillations. The fundamental harmonic whose period equals eight driving periods dominates the spectrum. We may treat it as a subharmonic (as an "undertone") of the driving oscillation. This harmonic describes the discussed above smooth component $\psi(t)$ of the compound period-8 oscillation.

The approximate approach based on the effective potential (see Fig. 2) for the slow motion provides a simple qualitative physical explanation for such an extraordinary and even counterintuitive behavior of the pendulum. Moreover, for subharmonic resonances with $n \gg 1$ this approach yields rather accurate quantitative results.

Indeed, since the natural slow oscillatory motion in the effective potential well is almost periodic, we suppose that a subharmonic resonance of order *n* can occur if one cycle of this slow motion covers approximately *n* driving periods. In other words, the driving frequency ω should be close to an integer multiple *n* of the natural frequency of slow oscillations near either the inverted or the ordinary equilibrium position: $\omega = n\omega_{\text{up}}$ or $\omega = n\omega_{\text{down}}$. In this case the phase locking can occur, in which one cycle of the slow motion is completed *exactly* during *n* driving periods. Synchronization of these modes with the oscillations of the pivot (phase locking) creates conditions for systematic supplying the pendulum with the energy needed to compensate for dissipation, and the whole process becomes exactly periodic.

As an example how the approach based on the effective potential allows us to explain properties of these *n*-periodic oscillations and to predict conditions at which they can occur, we consider first a simple special case

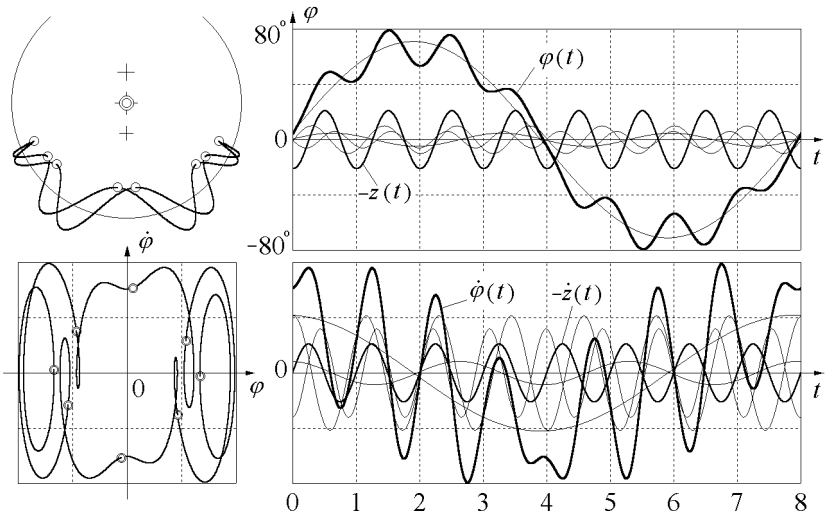

Figure 3. The spatial path, phase orbit with Poincaré sections, and graphs of stationary period-8 oscillations. The graphs are obtained by a numerical integration of the exact differential equation, Eqn. (2), for the momentary angular deflection $\varphi(t)$ (with $\omega_0 = 0$, $a/l = 0.265$, $Q = 400$). Time is indicated in drive periods. Thin lines show separate harmonics. The fundamental harmonic with the frequency $\omega/8$ dominates the spectrum. The 7th and 9th harmonics have nearly equal amplitudes. Graphs of the axis motion $-z(t)$ and $-\dot{z}(t)$ are also shown.

of the pendulum in the absence of gravity, or, which is essentially the same, the limiting case of very high driving frequencies $\omega \gg \omega_0$ ($\omega/\omega_0 \to \infty$). In this limit both equilibrium positions (ordinary and inverted) are equivalent, and the normalized driving amplitude $m = a/l$ is the only physical parameter to be predicted as a required condition for the subharmonic resonance of order n.

At $\omega_0 = 0$ (that is, in the absence of gravity), according to Eqn. (7), the frequency of slow oscillations is given by $\omega_{\text{slow}}/\omega = m/\sqrt{2}$, whence for the subharmonic resonance of order n, at which the period of the slow motion equals n periods of the axis, $m_{\min} = \sqrt{2}/(\omega/\omega_{\text{slow}}) = \sqrt{2}/n$. For the subharmonic resonance of 8th order ($n = 8$) shown in Fig. 3 we find $m_{\min} = \sqrt{2}/8 = 0.177$. This value is rather close to the predictions of a more precise theory of the boundaries for these modes based on the linearized differential equation of the system (see Eqn. (12) below), which gives for such period-8 small oscillations in the absence of gravity the normalized driving amplitude $a/l = 0.173$. The latter value agrees well with the simulation experiment in conditions of small angular excursions of the pendulum.

In the presence of gravity, assuming $\omega_{\text{down, up}} = \omega/n$ (n driving cycles during one cycle of the slow oscillation), we find for the minimum normalized driving amplitudes (for the boundaries of the subharmonic resonances) the values

$$m_{\min} = \sqrt{2\left(\frac{1}{n^2} \mp \frac{\omega_0^2}{\omega^2}\right)}, \tag{8}$$

Since negative values of ω_0^2 can be treated as referring to the inverted pendulum, the boundaries of subharmonic

resonances can be expressed both for the inverted and non-inverted pendulum by the same formula: $m_{\min} = \sqrt{2(1/n^2 - k)}$, where parameter $k = (\omega_0/\omega)^2$ is negative for the inverted pendulum. The limit of this expression at $n \to \infty$ gives the mentioned earlier approximate criterion of stability of the inverted pendulum (5): $m_{\min} = \sqrt{-2k}$ (where $k < 0$).

Being based on a decomposition of motion on slow oscillations and rapid vibrations with the driving frequency, Eqn. (8) is approximate and valid if the amplitude of constrained vibration of the axis is small compared to the pendulum's length ($a \ll l$). Moreover, in the presence of gravity the driving frequency must be much greater than the frequency of small natural oscillations of the pendulum ($\omega \gg \omega_0$). These restrictions mean that we should not expect from the approach discussed here to give an exhaustive description of the parametrically driven pendulum in all cases.

The simulations show clearly (see graphs in Fig. 3) that the momentary deflection angle $\varphi(t)$ can be represented approximately as a superposition of the slow varying mean angle $\psi(t)$ and the high frequency term whose angular amplitude is proportional to sine of $\psi(t)$:

$$\varphi(t) \approx \psi(t) - (z/l)\sin\psi(t) = \psi(t) - (a/l)\sin\psi(t)\cos\omega t. \tag{9}$$

For small angular excursions of the pendulum we can replace $\sin\psi$ by ψ in the second term of Eqn. (9), and assume for the slow motion the following sinusoidal time dependence: $\psi(t) = A\sin(\omega t/n)$ with the frequency ω/n. This means that the spectrum of small amplitude stationary n-period oscillations consists primarily of the fundamental harmonic $A\sin(\omega t/n)$ with the frequency ω/n, and two high harmonics of the orders $n-1$ and $n+1$:

$$\varphi(t) = A\sin(\frac{\omega}{n}t) - mA\sin(\frac{\omega}{n}t)\cos\omega t =$$

$$A\sin(\frac{\omega}{n}t) - \frac{mA}{2}\sin(\frac{n-1}{n}\omega t) + \frac{mA}{2}\sin(\frac{n+1}{n}\omega t). \tag{10}$$

This spectral composition is clearly seen from the plots in Fig. 3. While the pendulum is crossing the equilibrium position, both high harmonics add in opposite phases and thus almost don't distort the smooth motion (described by the principal harmonic). Near the utmost deflections, the phases of high harmonics coincide, and thus here their sum causes the most serious distortions of the smooth motion.

According to Eqn. (10), both high harmonics have equal amplitudes $mA/2$. However, we see from the plots in Fig. 3 that these amplitudes are slightly different. Therefore we can try to improve the approximate expression for $\varphi(t)$, Eqn. (10), as well as the theoretical values for the lower boundaries of subharmonic resonances, Eqn. (8), by assuming for the possible solution a similar spectrum but with unequal amplitudes, A_{n-1} and A_{n+1}, of the two high harmonics (for $n > 2$, the case of $n = 2$ will be considered separately):

$$\varphi(t) = A_1\sin(\frac{\omega}{n}t) + A_{n-1}\sin(\frac{n-1}{n}\omega t) + A_{n+1}\sin(\frac{n+1}{n}\omega t). \tag{11}$$

Since oscillations at the boundaries have infinitely small amplitudes, we can use instead of Eqn. (2) the following linearized (Mathieu) equation:

$$\ddot{\varphi} + 2\gamma\dot{\varphi} + (\omega_0^2 - m\omega^2 \sin\omega t)\varphi = 0. \tag{12}$$

Substituting $\varphi(t)$, Eqn. (11), into Eqn. (12) with $\gamma = 0$, and expanding the products of trigonometric functions, we obtain a system of approximate equations for the coefficients A_1, A_{n-1} and A_{n+1}:

$$\begin{aligned} 2(kn^2-1)A_1 + mn^2A_{n-1} - mn^2A_{n+1} &= 0, \\ mn^2A_1 + 2[n^2(k-1)+2n-1]A_{n-1} &= 0, \\ -mn^2A_1 + 2[n^2(k-1)-2n-1]A_{n+1} &= 0. \end{aligned} \tag{13}$$

The homogeneous system has a nontrivial solution if its determinant equals zero. This condition yields an equation for the corresponding critical (minimal) driving amplitude $m_{\min}$ at which n-period mode $\varphi(t)$, Eqn. (11), can exist. Solving the equation, we find:

$$m_{\min}^2 = \frac{2}{n^4}\frac{[n^6k(k-1)^2 - n^4(3k^2+1) + n^2(3k+2) - 1]}{[n^2(1-k)+1]}. \tag{14}$$

Then, for this critical driving amplitude $m_{\min}$, the fractional amplitudes A_{n-1}/A_1 and A_{n+1}/A_1 of high harmonics for a given order n can be easily found as the solutions to the homogeneous system of equations, Eqs. (13).

The limit of $m_{\min}$, Eqn. (14), at $n \to \infty$ gives an improved formula for the lower boundary of dynamic stabilization of the inverted position instead of the commonly known approximate criterion $m_{\min} = \sqrt{-2k}$, Eqn. (5):

$$m_{\min} = \sqrt{-2k(1-k)}, \qquad k = -(\omega_0/\omega)^2 = -g/(l\omega^2) < 0. \tag{15}$$

As follows from Eqn. (14), subharmonic oscillations of a given order n (for $n > 2$) are possible for $k \le 1/n^2$, that is, for the driving frequency $\omega \ge n\omega_0$. If the driving frequency ω is increased beyond the value $n\omega_0$ (i.e., as k is decreased from the critical value $1/n^2$ towards zero), the threshold driving amplitude rapidly increases. The limit of very high driving frequency ($\omega/\omega_0 \to \infty$), in which the gravitational force is insignificant compared with the force of inertia (or, which is essentially the same, the limit of zero gravity $\omega_0/\omega \to 0$), corresponds to $k = 0$. Negative k values describe the transition through zero gravity to the "gravity" directed upward, which is equivalent to the case of an inverted pendulum in ordinary (directed downward) gravitational field. Therefore for negative k values Eqn. (14) gives the threshold driving amplitudes for subharmonic resonances of the inverted pendulum.

Further details of subharmonic resonances are described in [21]. Here we would like to emphasize that subharmonic resonances, which have been discovered by Acheson (see [19]) in investigations of the dynamically

stabilized inverted pendulum with a vibrating pivot ("multiple-nodding" oscillations), are not specific for the inverted pendulum. They can be executed also (at appropriate values of the driving parameters) about the ordinary (downward) equilibrium position. Actually, the origin of subharmonic resonances is independent of gravity: similar "multiple-nodding" oscillations synchronized with the pivot can occur also in the absence of gravity about any of the two equivalent dynamically stabilized equilibrium positions. Since most peculiarities of these counter-intuitive modes are not related to the force of gravity, they can be physically explained when they are observed in their purest form in the absence of gravity, being described by Eqn. (2) with $\omega_0 = 0$.

According to Eqn. (14), the following values of the normalized driving amplitudes correspond to the threshold conditions at zero gravity ($k = 0$):

$$m_{\min} = \frac{\sqrt{2}(n^2-1)}{n^2\sqrt{n^2+1}}. \tag{16}$$

The fractional amplitudes A_{n-1}/A_1 and A_{n+1}/A_1 of the most important high harmonics of $\varphi(t)$ [expressed approximately by Eqn. (11)] for the case of zero gravity ($k = 0$) are given by the following formulas:

$$\frac{A_{n-1}}{A_1} = \frac{n+1}{\sqrt{2}\sqrt{n^2+1}(n-1)}, \quad \frac{A_{n+1}}{A_1} = \frac{n-1}{\sqrt{2}\sqrt{n^2+1}(n+1)}. \tag{17}$$

For subharmonic resonances of high orders ($n \gg 1$), Eqn. (16) yields the approximate value $m_{\min} \approx \sqrt{2}/n$ (in the case of zero gravity) obtained earlier with the help of the simple approach which explains the physical nature of n-order subharmonic resonance and treats its condition as the coincidence of n driving periods with one period of the smoothed, slow motion of the pendulum near the bottom of the effective potential well. The fractional amplitudes of both high harmonics A_{n-1}/A_1 and A_{n+1}/A_1, given by Eqn. (17), at $n \gg 1$ are almost equal and approach to the common value $1/(\sqrt{2}n) = m_{\min}/2$, in accordance with equation (10) that describes the n-period subharmonic oscillations as a superposition of the slow and rapid motions.

For the boundaries $m_{\min}$ of subharmonic resonances in cases of not very high orders n, Eqn. (16) gives improved theoretical values, as well as Eqn. (17) gives improved values for the (non-equal) fractional amplitudes of high harmonics A_{n-1}/A_1 and A_{n+1}/A_1. For the period-8 oscillations in the absence of gravity ($\omega_0 = 0$), Eqn. (16) yields for the critical value of the driving amplitude $a/l = m_{\min} = 63/(32\sqrt{130}) = 0.173$. Equations (17) yield for the fractional contributions of the 7th and 9th harmonics $A_7/A_1 = 9/(7\sqrt{130}) = 0.113$, $A_9/A_1 = 7/(9\sqrt{130}) = 0.068$. All these theoretical values agree perfectly well with the simulations of period-8 small oscillations based on numerical integration of the exact differential equation of the system, Eqn. (2). We have observed also a perfect agreement between theoretical and experimental results for subharmonic resonances with smaller values of n.

4 Overlapping of subharmonic resonances and their spectral composition

If the drive amplitude exceeds the threshold value for some subharmonic resonance of order n given by Eqn. (14), the pendulum, being excited to this mode, executes in its slow motion finite angular excursions over the

slanting slopes of the effective potential well, Fig. 2. Due to non-parabolic shape of the potential well, this slow motion $\psi(t)$ is not purely sinusoidal, contrary to our assumption used in Eqn. (10). This causes the appearance of additional spectral components. For the oscillations of a large swing shown in Fig. 3, the contribution of the 3rd harmonic to the spectrum is noticeable. Moreover, because the smooth motion is executed in the effective potential well with a "soft" restoring force, the period becomes longer as the amplitude is increased. Therefore large-amplitude period-8 oscillations shown in Fig. 3 (their swing equals 80°) occur at a considerably greater value of the driving amplitude ($a = 0.265\,l$) than the critical (threshold) value $a_{\min} = 0.173\,l$.

By virtue of the mentioned above dependence of the period of non-harmonic smooth motion on the swing, several modes of subharmonic resonance with different values of n can coexist at the same amplitude and frequency of the pivot. Indeed, the period of a slow non-harmonic oscillation with some finite amplitude can be equal to, say, six driving periods, while the period of a slow oscillation with a somewhat greater amplitude in the same non-parabolic potential well can be equal to eight driving periods.

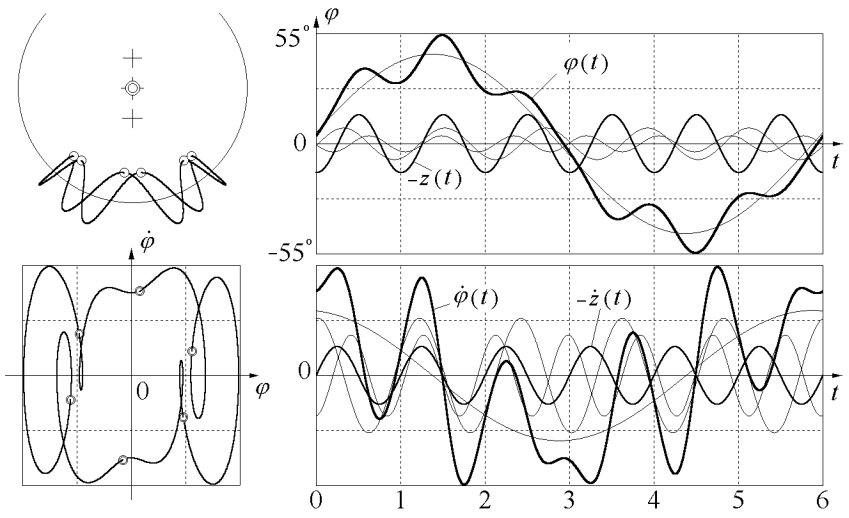

Figure 4. The spatial path, phase orbit with Poincaré sections, and graphs of stationary period-6 oscillations. The graphs are obtained by a numerical integration of the exact differential equation, Eqn. (2), for the momentary angular deflection $\varphi(t)$ (with $\omega_0 = 0$, $a/l = 0.265$, $Q = 400$). Thin lines show separate harmonics. The fundamental harmonic with the frequency $\omega/6$ dominates the spectrum. The 5th and 7th harmonics have noticeable amplitudes. Graphs of the axis motion $-z(t)$ and $-\dot{z}(t)$ are also shown.

Figure 4 shows the simulation of such period-6 mode, coexisting with the mode shown in Fig. 3 (obtained at identical parameters of the system). That is, both smooth motions occur in the same effective potential well. In which of these competing modes is the pendulum eventually trapped in a certain simulation, depends on the starting conditions. The set of initial conditions that leads, after transients decay, to a given dynamic equilibrium (to the same steady-state periodic motion, or attractor) in the limit of large time, constitutes the basin of attraction of this attractor. The coexisting periodic motions in Figs. 3 and 4 represent competing attractors and are characterized by different domains of attraction. The influence of the non-linear character of Eqn. (3) for the slow motion of the pendulum on the critical driving amplitude and spectral composition of resonant oscillations is discussed

in [21] with more detail.

Friction introduces a phase shift between forced oscillations of the pivot and harmonics of the steady-state n-periodic motion of the pendulum. By virtue of this phase shift the pendulum is supplied with energy needed to compensate for frictional losses. With friction, the direct and backward spatial paths of the pendulum do not coincide, and the symmetry of the phase trajectory with respect to the ordinate axis is destroyed. This is clearly seen from Figs. 3 or 4 for subharmonic resonances in the presence of weak friction.

5 Subharmonic resonances of fractional orders

In this section, we discuss new modes of regular behavior of the parametrically driven pendulum, akin to the above-described subharmonic resonances. We have discovered these modes in simulation experiments and briefly described for the first time in [21].

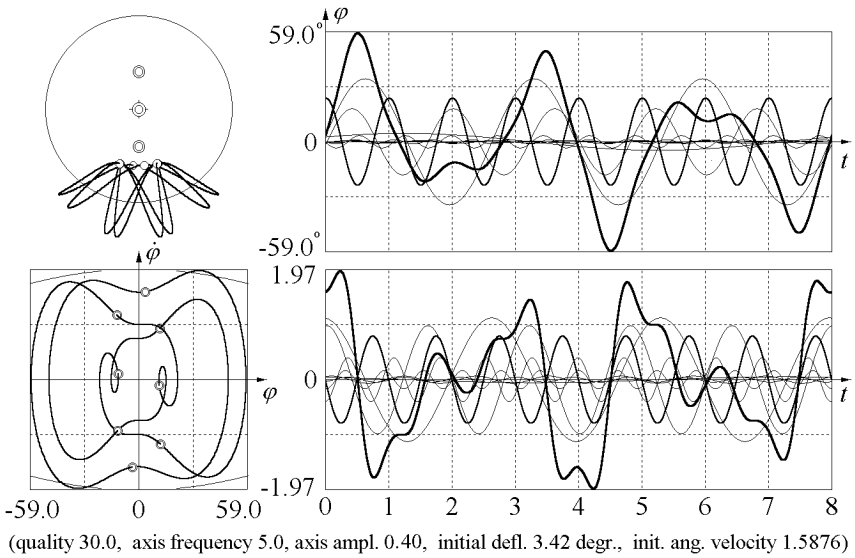

Figure 5. The spatial path, phase orbit, and graphs of stationary oscillations that can be treated as a subharmonic resonance of a fractional order 8/3. The third harmonic (frequency $3\omega/8$) dominates the spectrum.

Figure 5 shows a regular period-8 motion of the pendulum, which can be characterized as a subharmonic resonance of a fractional order, specifically, of the order 8/3 in this example. Here the amplitude of the fundamental harmonic (whose frequency equals $\omega/8$) is much smaller than the amplitude of the third harmonic (frequency $3\omega/8$). This third harmonic dominates the spectrum, and can be regarded as the principal one, while the fundamental harmonic can be regarded as its third subharmonic. Considerable contributions to the spectrum are given also by the 5th and 11th harmonics of the fundamental frequency. Approximate boundary conditions for small-amplitude stationary oscillations of this type ($n/3$-order subresonance) can be found analytically from the linearized differential equation by a method similar to that used above for n-order subresonance: we can try as $\varphi(t)$ a solution consisting of spectral components with frequencies $3\omega/n$, $(n-3)\omega/n$, and $(n+3)\omega/n$:

$$\varphi(t) = A_3 \sin(\frac{3}{n}\omega t) + A_{n-3} \sin(\frac{n-3}{n}\omega t) + A_{n+3} \sin(\frac{n+3}{n}\omega t). \quad (18)$$

Substituting this trial function $\varphi(t)$ into Eqn. (12) (with $\gamma = 0$) and expanding the products of trigonometric functions, we obtain a system of equations for the coefficients A_3, A_{n-3} and A_{n+3}. Condition of existence of a non-trivial solution to the system yields the following expression for the minimal driving amplitude:

$$m_{\min} = \frac{3\sqrt{2}(n^2 - 3^2)}{n^2\sqrt{n^2 + 3^2}}. \quad (19)$$

(Compare Eqn. (19) with a similar expression, Eqn. (16), for the critical driving amplitude of the integer-order subharmonic resonances.) The analytical results of calculations for $n \geq 8$ agree well with the simulations, especially if one more high harmonic is included in the trial function $\varphi(t)$, Eqn. (18). If the driving amplitude exceeds the critical value, the angular excursion of the pendulum at these modes increases, and additional harmonics appear in its spectrum.

6 Principal parametric resonance and the upper boundary of stability in the inverted state

For principal parametric resonance, two driving cycles are executed during one period of stationary oscillations. This means that we can treat it as a subharmonic resonance of the second order ($n = 2$). For small n values the effective potential approach is not applicable because in such cases the period of "smooth" motion contains only a few driving periods. The "fast" component of motion, whose frequency for $n = 2$ is only twice the driving frequency, is not fast enough for good averaging in transition to the effective potential. Although in this case we cannot use the effective potential, the physical explanation of instability of the the downward position (which leads to excitation of principal parametric resonance) is quite straightforward. Also the quantitative theoretical expressions for the boundaries of the instability region in the plane $\omega - m$ (driving frequency – drive amplitude) are easily available with the help of standard methods (see, for example, [3]).

However, the treatment of principal parametric resonance as a subharmonic resonance of a definite order $n = 2$ leads us to the conclusion that a similar phenomenon is possible not only for the downward position of the pendulum, but also for the dynamically stabilized inverted pendulum, as well as for the pendulum with oscillating axis in the absence of gravity, just like the above-discussed subharmonic resonances with $n > 2$ are possible in all these cases. Indeed, when the amplitude a of the pivot vibrations is increased beyond certain critical value $a_{\max}$, the dynamically stabilized inverted position of the pendulum loses its stability. After a disturbance the pendulum does not come to rest in the up position, no matter how small the release angle, but instead eventually settles into a finite amplitude steady-state oscillation about the vertical position at frequency $\omega/2$ (half the driving frequency). This loss of stability of the inverted pendulum has been first described by Blackburn *et al.* [8] (the "flutter" mode) and demonstrated experimentally in [9]. (The latest numerical investigation of the bifurcations associated with the stability of the inverted state can be found in [18].) Next we show that this "flutter" mode and ordinary parametric resonance of the pendulum in the downward position belong to the same branch (in the parameters plane $\omega - m$) of possible stationary oscillations.

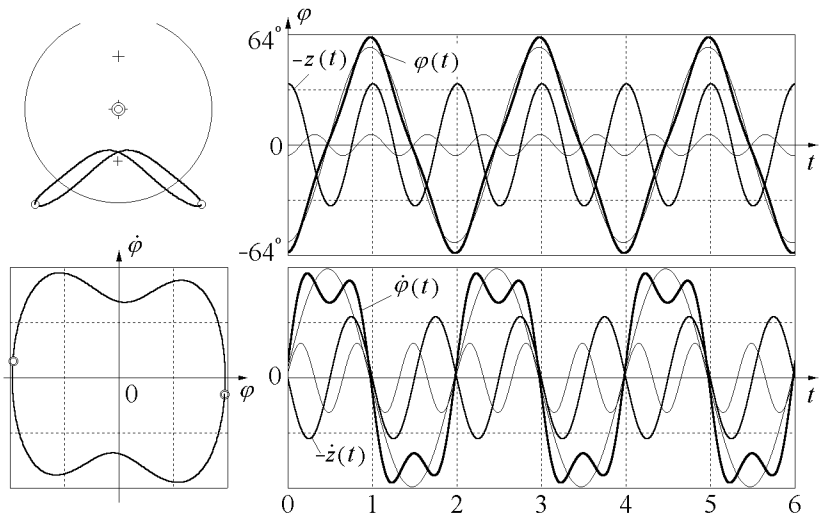

Figure 6. Stationary double-period oscillations occurring over the upper boundary of dynamic stability in the absence of gravity (the "flutter" mode). The spectrum consists of the fundamental harmonic (frequency $\omega/2$) and the third harmonic (frequency $3\omega/2$). The graphs are obtained by a numerical integration of the exact differential equation for the momentary angular deflection $\varphi(t)$, Eqn. (2) with $\omega_0 = 0$, $a/l = 0.56$, $Q = 10.0$.

The graphs and the double-lobed phase trajectory of such oscillations are shown in Fig. 6. The simulation shows a very simple spectral composition: the fundamental harmonic whose frequency equals $\omega/2$ (half the driving frequency ω) with an addition of the third harmonic with the frequency $3\omega/2$. Therefore the boundary of dynamic stability can be found directly from the linearized differential equation of the system, Eqn. (12), by including these harmonics into the trial function:

$$\varphi(t) = A_1 \cos(\omega t/2) + A_3 \cos(3\omega t/2). \tag{20}$$

Thus we get a system of homogeneous equations for the coefficients A_1 and A_3, which has a nontrivial solution when its determinant equals zero. This requirement yields a quadratic equation for the desired normalized critical driving amplitude $a_{\max}/l = m_{\max}$. The relevant root of this equation (in the case $\omega_0 = 0$ which corresponds to the absence of gravity or to the high frequency limit of the pivot oscillations with gravity) is $m_{\max} = 3(\sqrt{13} - 3)/4 = 0.454$, and the corresponding ratio of amplitudes of the third harmonic to the fundamental one equals $A_3/A_1 = (\sqrt{13} - 3)/6 = 0.101$.

A somewhat more complicated calculation in which the higher harmonics (up to the 7th) in $\varphi(t)$ are taken into account yields for $m_{\max}$ and A_3/A_1 the values that coincide (within the assumed accuracy) with those cited above. These values agree well with the simulation experiment in conditions of the absence of gravity ($\omega_0 = 0$) and very small angular excursion of the pendulum. When the normalized amplitude of the pivot $m = a/l$ exceeds the critical value $m_{\max} = 0.454$, the swing of the period-2 "flutter" oscillation (amplitude A_1 of the fundamental harmonic) increases in proportion to the square root of this excess: $A_1 \propto \sqrt{a - a_{\max}}$. This dependence follows from the nonlinear differential equation of the pendulum, Eqn. (2), if $\sin\varphi$ is approximated as $\varphi - \varphi^3/6$, and agrees well with simulation experiments for amplitudes up to 45°.

As the normalized amplitude $m = a/l$ of the pivot is increased over the value 0.555, the symmetry-breaking bifurcation occurs: The angular excursions of the pendulum to one side and to the other become different, destroying the spatial symmetry of the oscillation and hence the symmetry of the phase orbit. As the pivot amplitude is increased further, after $m = 0.565$ the system undergoes a sequence of period-doubling bifurcations, and finally, at $m = 0.56622$ (for $Q = \omega/2\gamma = 20$), the oscillatory motion of the pendulum becomes replaced, at the end of a very long chaotic transient, by a regular unidirectional period-1 rotation.

Similar theoretical investigation of the boundary conditions for period-2 stationary oscillations in the presence of gravity allows us to obtain the dependence of the critical (destabilizing) amplitude $m = a/l$ of the pivot on the driving frequency ω. In terms of $k = \pm(\omega_0/\omega)^2$ this dependence has the following form:

$$m_{\max} = (\sqrt{117 - 232k + 80k^2} - 9 + 4k)/4. \tag{21}$$

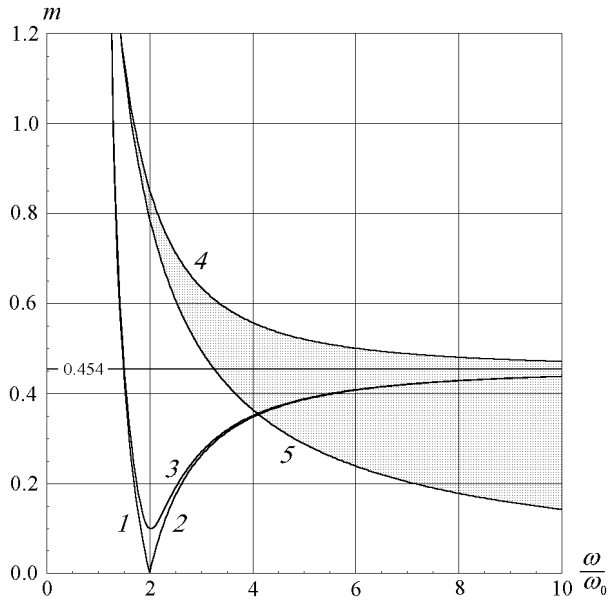

Figure 7. The boundaries of parametric instability – driving amplitude $m = a/l$ versus normalized driving frequency. *1* and *2* – boundaries of the principal interval of parametric instability ($\omega \approx 2\omega_0$) for the non-inverted pendulum in the absence of friction, *3* – the same with friction ($Q = 5.0$), *4* and *5* – the upper and lower boundaries of dynamic stability for the inverted pendulum.

The diagram in Fig. 7 shows these boundaries of instability. For the downward position of the pendulum, in the absence of friction the critical amplitude given by Eqn. (21) tends to zero as the frequency of the pivot approaches $2\omega_0$ from either side (curves *1* and *2*). This case (small vertical oscillations of the pivot with the frequency approximately twice the natural frequency of the pendulum) corresponds to ordinary parametric resonance, for which a very clear physical explanation can be suggested. If the driving frequency deviates from $2\omega_0$, a finite

driving amplitude is required for infinitely small steady parametric oscillations even in the absence of friction. Curve *3* shows in the parameters plane (ω/ω_0, a/l) the region of principal parametric resonance with friction (for $Q = 5.0$). The non-inverted vertical position of the pendulum with the pivot vibrating at frequency $2\omega_0$ loses stability when the normalized amplitude of this vibration exceeds the threshold value of $1/2Q$. This curve almost merges with curves *1* and *2* as the frequency ω deviates from the resonant value $2\omega_0$. In the high-frequency limit, for which the role of gravity is negligible, the normalized critical pivot amplitude a/l tends to the above-indicated value $a/l = 3(\sqrt{13} - 3)/4 = 0.454$ that corresponds to the destabilization of the two symmetric equilibrium positions in the absence of gravity.

Curve *4* of this diagram corresponds to destabilization of the inverted pendulum by excitation of the "flutter" oscillations. The smaller the frequency of the pivot, the greater the critical amplitude at which the inverted position becomes unstable. We note that this curve *4* is essentially the continuation (through infinite values of the driving frequency) of the same branch (curve *2* without friction or curve *3* with friction) of period-2 steady-state oscillations corresponding to the boundaries of instability with respect to excitation of the ordinary parametric resonance of the non-inverted pendulum. This proves the close relationship between the parametric instability of the non-inverted pendulum (ordinary parametric resonance) and the upper limit of the dynamic stability of the inverted pendulum (the "flutter" oscillations).

Curve *5* in Fig. 7 shows the lower boundary of dynamic stabilization of the inverted pendulum, given by the improved criterion, Eqn. (15). In case of small drive amplitudes, the loss of stability at crossing this boundary occurs when the effective potential well corresponding to the inverted position has zero depth. Thus, the region of stability of the inverted pendulum occupies the shaded part of the parameter plane between curves *5* and *4*.

7 Complicated modes of regular behavior

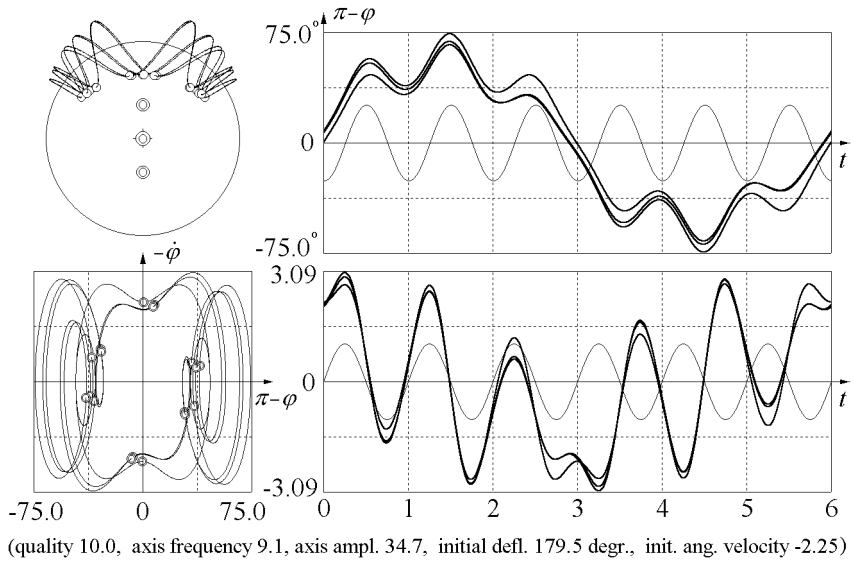

Figure 8. The spatial path, phase orbit, and graphs of period-18 oscillations.

One more type of regular behavior is shown in Fig. 8. This mode can be characterized as resulting from

a period multiplication of a subharmonic resonance, specifically, in this example, as tripling of the six-order subresonance. Comparing this figure with Fig. 4, we see that in both cases the motion is quite similar during any cycle of six consecutive driving periods each, but in Fig. 8 the motion during each next cycle of six periods is slightly different from the preceding cycle. After three such cycles (of six driving periods each) the phase orbit becomes closed and then repeats itself, so the period of this stationary motion equals 18 driving periods. However, the harmonic component whose period equals six driving periods dominates the spectrum (just like in the spectrum of period-6 oscillations in Fig. 4), while the fundamental harmonic (frequency $\omega/18$) of a small amplitude is responsible only for tiny divergences between the adjoining cycles, each consisting of six driving periods.

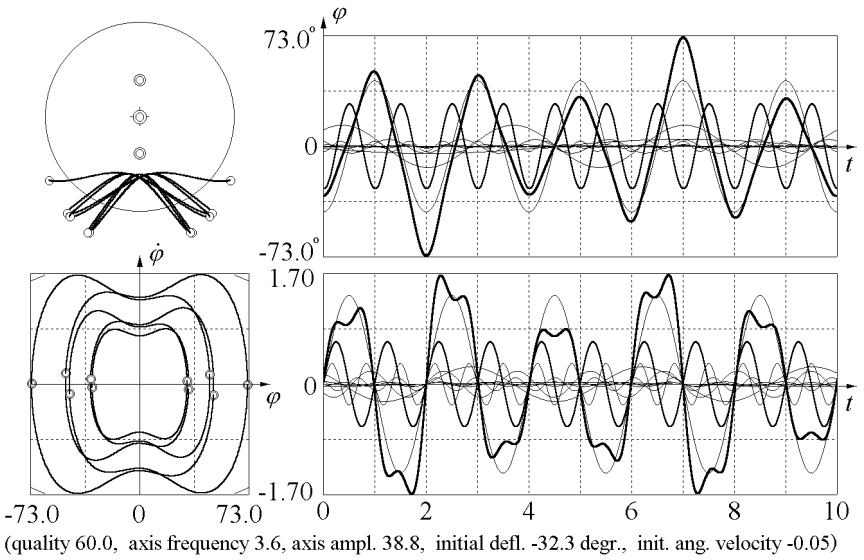

Figure 9. The spatial path, phase orbit, and graphs of period-10 oscillations.

Such multiplications of the period are characteristic of large amplitude oscillations at subharmonic resonances both for the inverted and downward positions of the pendulum. Figure 9 shows a stationary oscillation with a period that equals ten driving periods. This large amplitude motion can be treated as originating from a period-2 oscillation (that is, from ordinary principal parametric resonance) by a five-fold multiplication of the period. The harmonic component with half the driving frequency ($\omega/2$) dominates the spectrum. But in contrast to the preceding example, the divergences between adjoining cycles consisting of two driving periods each are generated by the contribution of a harmonic with the frequency $3\omega/10$ rather than the fundamental harmonic (frequency $\omega/10$) whose amplitude is much smaller.

One more example of complicated steady-state oscillation is shown in Fig. 10. This period-30 motion can be treated as generated from the period-2 principal parametric resonance first by five-fold multiplication of the period (resulting in period-10 oscillation), and then by next multiplication (tripling) of the period. Such large-period stationary regimes are characterized by small domains of attraction consisting of several disjoint islands of initial states on the phase plane. We note that it is impossible to excite these modes by a slow variation (scanning) of a control parameter during the motion which started in some other mode: when all the parameters assume the

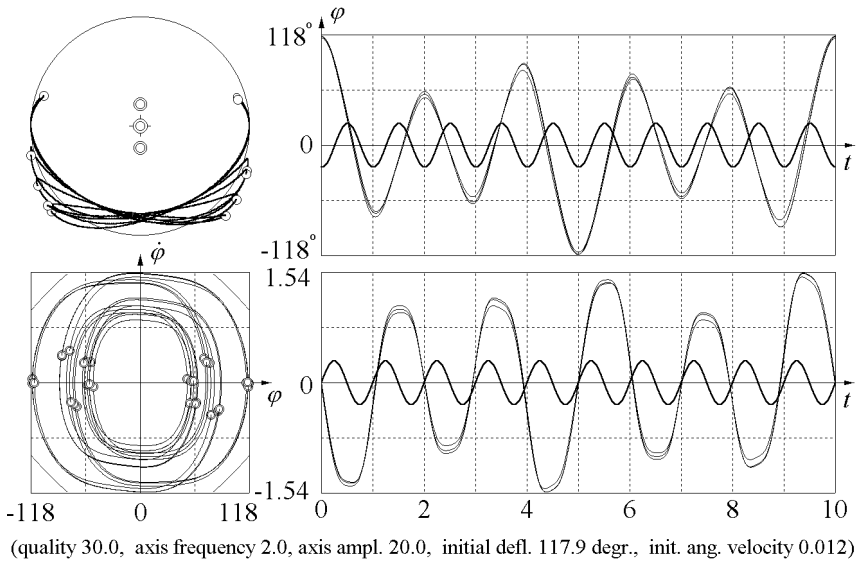

Figure 10. The spatial path, phase orbit, and graphs of period-30 oscillations.

values required for such long-period regime, the pendulum occurs as a rule in a different (usually rather simple) coexisting mode.

Other modes of regular behavior are formed by unidirectional period-2 or period-4 (or even period-8) rotation of the pendulum or by oscillations alternating with revolutions to one or to both sides in turn. Such modes have periods constituting several driving periods.

8 New modes of chaotic behavior

At large driving amplitudes the pendulum exhibits various chaotic regimes. Chaotic behavior of nonlinear systems has been a subject of intense interest during recent decades, and the forced pendulum is an excellent physical model for studying general laws of the dynamical chaos [13] – [18], [22] – [24].

Next we describe several different kinds of chaotic regimes, which, as far as we know, have not been discussed in the literature. Poincaré mapping, that is, a stroboscopic picture of the phase plane for the pendulum taken once during each driving cycle after initial transients have died away, gives an obvious and convenient means to distinguish between regular periodic behavior and persisting chaos. A steady-state subharmonic of order n would be seen in the Poincaré map as a systematic jumping between n fixed mapping points. When the pendulum motion is chaotic, the points of Poincaré sections wander randomly, never exactly repeating. Their behavior in the phase plane gives an impression of the strange attractor for the motion in question.

Figure 11 shows an example of a purely oscillatory two-band chaotic attractor for which the set of Poincaré sections consists of two disjoint islands. This attractor is characterized by a fairly large domain of attraction in the phase plane. The two islands of the Poincaré map are visited regularly (strictly in turn) by the representing point, but within each island the point wanders irregularly from cycle to cycle. This means that for this kind of motion the flow in the phase plane is chaotic, but the distance between any two initially close phase points within this attractor remains limited in the progress of time: The greatest possible distance in the phase plane is determined by the size of these islands of the Poincaré map.

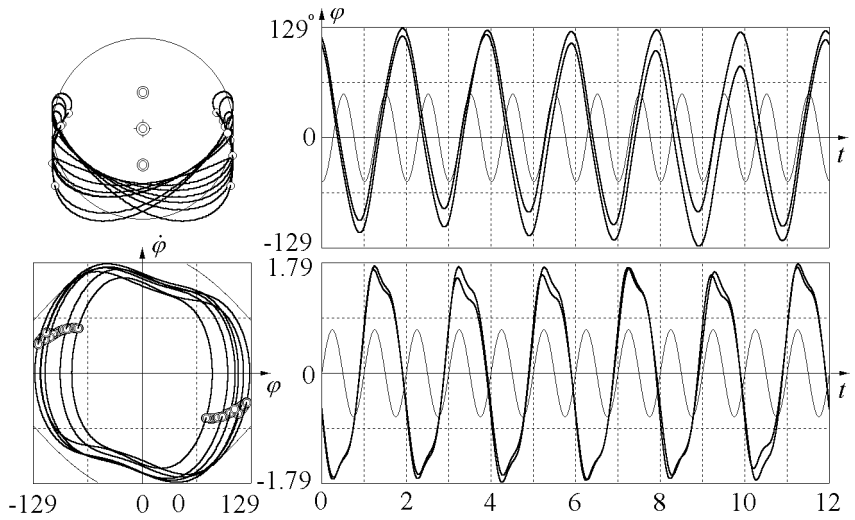

(quality 3.1, axis frequency 1.8, axis ampl. 40.0, initial defl. 118.8 degr., init. ang. velocity -0.534)

Figure 11. Chaotic attractor with a two-band set of Poincaré sections.

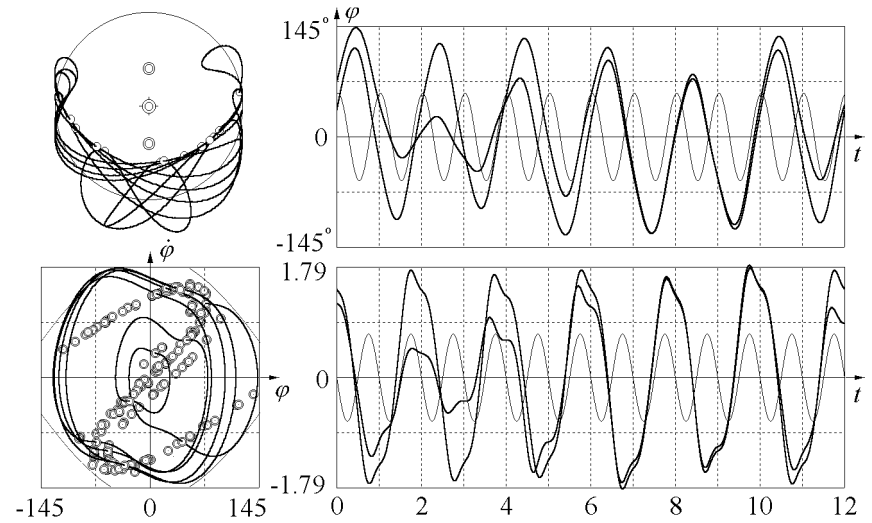

(quality 3.2, axis frequency 1.8, axis ampl. 40.0, initial defl. 75.28 degr., init. ang. velocity 1.21486)

Figure 12. Chaotic attractor with a strip-like set of Poincaré sections.

Figure 12 shows the chaotic attractor that corresponds to a slightly reduced friction, while all other parameters are unchanged. Gradual reduction of friction causes the islands of Poincaré sections to grow and coalesce, and to form finally a strip-shaped set occupying considerable region of the phase plane. As in the preceding example, each cycle of these oscillations (consisting of two driving periods) slightly but randomly varies from the preceding one. However, in this case, the large and almost constant amplitude of oscillations occasionally (after a large but unpredictable number of cycles) considerably reduces or, vice versa, increases (sometimes so that the pendulum makes a full revolution over the top). These decrements and increments result sometimes in switching the phase

of oscillations: the pendulum motion, say, to the right side that occurred during even driving cycles is replaced by the motion in the opposite direction. During long intervals between these seldom events, the motion of the pendulum is purely oscillatory with only slightly (and randomly) varying amplitude. This kind of intermittent irregular behavior differs from the well-known so-called tumbling chaotic attractor that exists over a relatively broad range of the parameter space [22]. The tumbling attractor is characterized by random oscillations (whose amplitude varies strongly from cycle to cycle), often alternated with full revolutions to one or the other side.

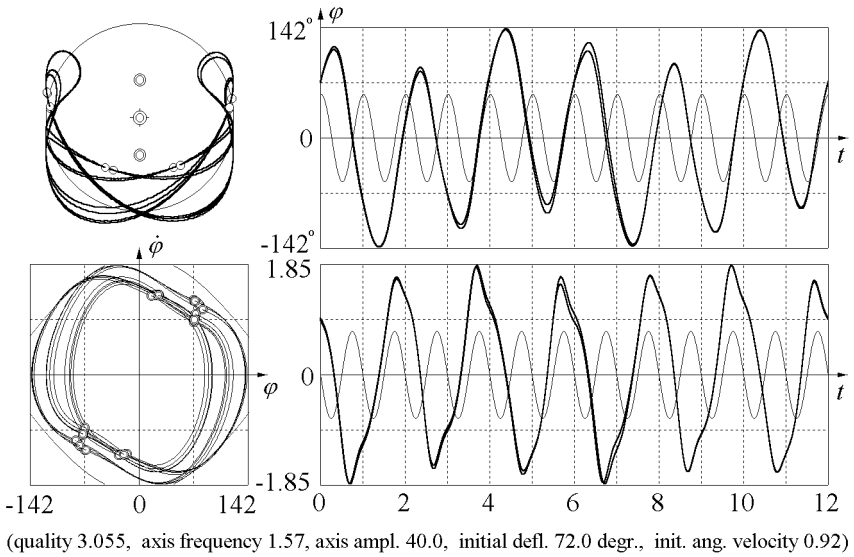

Figure 13. An oscillatory six-band chaotic attractor.

Figure 13 illustrates one more kind of strange attractors. In this example the motion is always purely oscillatory, and nearly repeats itself after each six driving periods. The six bands of Poincaré sections make two groups of three isolated islands each. The representing point visits these groups in alternation. It also visits the islands of each group in a quite definite order, but within each island the points continue to bounce from one place to another without any apparent order. The six-band attractor has a rather extended (and very complicated in shape) domain of attraction. Nevertheless, at these values of the control parameters the system exhibits multiple asymptotic states: The chaotic attractor coexists with several periodic regimes.

Chaotic regimes exist also for purely rotational motions. Poincaré sections for such rotational chaotic attractors can make several isolated islands in the phase plane. A possible scenario of transition to such chaotic modes from unidirectional regular rotation lies through an infinite sequence of period-doubling bifurcations occurring when a control parameter (the driving amplitude or frequency or the braking frictional torque) is slowly varied without interrupting the motion of the pendulum. However, there is no unique route to chaos for more complicated chaotic regimes described above.

9 Concluding remarks

The parametrically excited pendulum is richer in various modes of possible behavior than we can expect for such a simple physical system. Most of these modes can hardly be called “simple.” In this paper we have touched

only a small part of existing motions. We have suggested a clear physical explanation of subharmonic resonances and developed an approximate quantitative theory of these modes. The spectral composition of subharmonic resonances is investigated quantitatively, and their low-amplitude boundaries in the parameter space are determined. Several related modes of regular behavior (subharmonic resonances of fractional orders) are described and explained for the first time. We have shown also that "flutter" mode (destabilization of the dynamically stabilized inverted pendulum) has common physical roots with ordinary parametric resonance (instability of the downward position of the pendulum).

The simulations show that variations of the parameter set (dimensionless driving amplitude a/l, normalized driving frequency ω/ω_0, and quality factor Q) result in numerous different regular and chaotic types of behavior. The pendulum's dynamics exhibits a great variety of other asymptotic rotational, oscillatory, and combined (both rotational and oscillatory) multiple-periodic stationary states as well as chaotic attractors, whose basins of attraction are characterized by a surprisingly complex (fractal) structure. Computer simulations reveal also intricate sequences of bifurcations, leading to numerous complicated chaotic regimes. Most of such motions that we observed in simulations remained beyond the scope of this paper. They are still waiting for plausible physical explanations. With good reason we can suppose that this seemingly simple physical system is almost inexhaustible.

REFERENCES

[1] A. Stephenson, "On an induced stability," Phil. Mag. **15**, 233 – 236 (1908).

[2] P. L. Kapitza, "Dynamic stability of the pendulum with vibrating suspension point," Soviet Physics – JETP **21**, (5) 588 – 597 (1951) (in Russian), see also "Collected papers of P. L. Kapitza," edited by D. Ter Haar, Pergamon, London (1965), v. 2, pp. 714 – 726.

[3] L. D. Landau and E. M. Lifschitz, "Mechanics," Nauka Publishers, Moscow (1988) (in Russian), "Mechanics," Pergamon, New York (1976) pp. 93 - 95.

[4] F. M. Phelps, III and J. H. Hunter, Jr. "An analytical solution of the inverted pendulum," Am. J. Phys. **33**, 285 – 295 (1965), **34**, 533 – 535 (1966).

[5] D. J. Ness, "Small oscillations of a stabilized, inverted pendulum," Am. J. Phys. **35**, 964 – 967 (1967).

[6] H. P. Kalmus, "The inverted pendulum," Am. J. Phys. **38**, 874 – 878 (1970).

[7] M. M. Michaelis, "Stroboscopic study of the inverted pendulum," Am. J. Phys. **53**, (11) 1079 – 1083 (1985).

[8] James A. Blackburn, H. J. T. Smith, N. Groenbech-Jensen, "Stability and Hopf bifurcations in an inverted pendulum," Am. J. Phys. **60**, (10) 903 – 908 (1992).

[9] H. J. T. Smith, J. A. Blackburn, "Experimental study of an inverted pendulum," Am. J. Phys. **60**, (10) 909 – 911 (1992).

[10] Michael J. Moloney, "Inverted pendulum motion and the principle of equivalence," Am. J. Phys. **64**, (11) 1431 (1996).

[11] W. T. Grandy, Jr., Matthias Schöck, "Simulations of nolinear pivot-driven pendula," Am. J. Phys. **65**, (5) 376 – 381 (1997).

[12] Julia G. Fenn, Derek A. Bayne, and Bruce D. Sinclair, "Experimental investigation of the 'effective potential' of an inverted pendulum," Am. J. Phys. **66**, (11) 981 – 984 (1998).

[13] John B. McLaughlin, "Period-doubling bifurcations and chaotic motion for a parametrically forced pendulum," J. Stat. Physics **24**, (2) 375 – 388 (1981)

[14] B. P. Koch, R. W. Leven, B. Pompe, and C. Wilke, "Experimental evidence for chaotic behavior of a parametrically forced pendulum," Phys. Lett. A **96**, (5) 219 – 224 (1983)

[15] R. W. Leven, B. Pompe, C. Wilke, and B. P. Koch, “Experiments on periodic and chaotic motions of a parametrically forced pendulum,” Physica D **16**, (3) 371 – 384 (1985)
[16] Willem van de Water and Marc Hoppenbrouwers, Freddie Christiansen, “Unstable periodic orbits in the parametrically excited pendulum,” Phys. Rev. A **44**, (10) 6388 - 6398 (1991)
[17] John Starrett and Randall Tagg, “Control of a chaotic parametrically driven pendulum,” Phys. Rev. Lett. **74**, (11) 1974 – 1977 (1995)
[18] Sang-Yoon Kim and Bambi Hu, “Bifurcations and transitions to chaos in an inverted pendulum,” Phys. Rev. E **58**, (3) 3028 – 3035 (1998)
[19] D. J. Acheson, “Multiple-nodding oscillations of a driven inverted pendulum,” Proc. Roy. Soc. London **A 448**, 89 – 95 (1995)
[20] E. I. Butikov, “On the dynamic stabilization of an inverted pendulum,” Am. J. Phys. **69**, (7), 755 – 768 (2001)
[21] E. I. Butikov, “Subharmonic Resonances of the Parametrically Driven Pendulum,” Journal of Physics A: Mathematical and General, **35** pp. 6209 - 6231 (2002).
[22] M. J. Clifford and S. R. Bishop, “Inverted oscillations of a driven pendulum,” Proc. Roy. Soc. London A **454**, 2811 – 2817, (1998).
[23] D. J. Sudor, S. R. Bishop, “Inverted dynamics of a tilted parametric pendulum,” Eur. J. Mech. A/Solids, **18**, 517 – 526 (1999).
[24] S. R. Bishop, D. J. Sudor, “The ‘not quite’ inverted pendulum,” Int. Journ. Bifurcation and Chaos, **9** (1), 273 – 285 (1999).